Rolling contact fatigue
Damage function development from two-disc test data
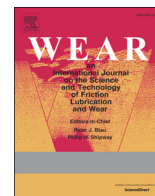
Hiensch, Martin; Burgelman, Nico

Important note
To cite this publication, please use the final published version (if applicable).
Please check the document version above.

Rolling contact fatigue: Damage function development from two-disc test data

Martin Hiensch[a,b,*], Nico Burgelman[b]

[a] Delft University of Technology, Section of Railway Engineering, Faculty of Civil Engineering and Geosciences, Stevinweg 1, 2628 CN Delft, the Netherlands
[b] DEKRA Rail, Concordiastraat 67, 3551 EM, Utrecht, the Netherlands

A B S T R A C T

The concept of the rail damage function provides vital understanding of the operational performance of rail grades in terms of surface degradation. Previously, material specific damage functions have been derived from measurements in track combined with vehicle-track simulations. However, from the occurring wide range in track loading conditions it is difficult to achieve clear characterisation results from track data only.

To reach more controlled loading conditions, a rolling-sliding two-disc laboratory set up could be applied. The validation of a two-disc test approach in order to define rail/wheel interface wear and RCF response is the topic of the here presented study.

1. Introduction

Rail damage functions describe the operational performance/degradation of the rail running surface in dependence on the loading conditions imposed by the railway vehicle and rail grade. When damage functions are available for a wide range of rail grades, the track engineer can select the most appropriate rail grade for use at a given location, considering the loading levels and loading frequencies for that particular site.

Work has been undertaken in developing a parameter capable of describing damage development associated with RCF. Burstow [1] has found the wear energy number (Tγ) to provide the best correlation between RCF damage simulation work and observed crack location in the field. Tγ is a measure of the energy dissipated within the wheel-rail contact, describing the amount of energy which would be available for initiating and propagating damage at the rail head. A material specific damage function is presented in Ref. [1], derived from track observations in combination with related vehicle-track simulations. The in Ref. [2] presented study extends this concept from conventional pearlitic rail to premium rail. From the occurring wide range in loading conditions in track (e.g. due to different vehicle types, wheel profiles, vehicle speed, traction, adhesion levels), it is difficult to achieve clear characterisation results from track observations only. To obtain more controlled conditions, experimental two-disc machines are used in laboratories to investigate the wheel-rail interface, substituting the rail by one of the discs. This approach could be applied to both establish and validate the damage functions for the different materials and to understand the relationship between material properties and the RCF damage index to serve future rail grade development. The validation of the two-disc test approach in order to define rail/wheel interface wear and RCF response to Tγ loading levels is the topic of the here presented study.

The development of a two-disc test rig for testing rolling-sliding contact under closely controlled conditions has been presented in Refs. [3,4]. It has been shown that the set-up allows the contact to be examined over a wide range of loads, speeds and slip ratios. RCF and wear behaviour of rail and wheel materials have been studied by means of two disc testing, among others in Refs. [5,6]. Initiation and growth of RCF cracks has been achieved during these tests, showing that the initiation of surface cracks to take place if the surface layer accumulates uni-directional plastic strain higher than the strain to failure. Other researches [15,16] demonstrated how factors such as rolling direction, angle of attack and contact pressure distribution affects the RCF of wheel/rail materials. Daves et al. [17] presents a two-dimensional wheel/rail contact model predicting the crack growth direction considering stick-slip behaviour of wheel/rail contact. Related metallographic investigations of a rail on a full scale test-rig suggest that the angle of the deformation lines decides if a crack grows parallel to the surface and will be removed as wear particle in further contacts or develops as a crack following the deformation line. In search of

---

* Corresponding author. Delft University of Technology, Section of Railway Engineering, Faculty of Civil Engineering and Geosciences, Stevinweg 1, 2628 CN, Delft, the Netherlands.

E-mail address: e.j.m.hiensch@tudelft.nl (M. Hiensch).

improved lifetime performance many two-disc studies focus on describing the wear behaviour with regard to specific loading conditions. The aim of this study is to determine if the RCF-damage function can be derived from two-disc testing, addressing both the RCF and wear dominated regime.

Since two-disc machines often are scaled models, scaling factors of the involved physical laws need to be determined and respected in order to validly analyse the phenomena considered. Different researchers [7–9] have studied the effect of scaling and simulation of the wheel-roller contact instead of the wheel-rail contact. With respect to the creep forces, Jaschinsky [7] concludes shape similarity of the contact ellipse to be important when the creep forces are not saturated. Tγ is found to scale proportional to the normal force. In Ref. [10] Bosso conducts a comparison between the different scaling methods/factors, discussing the kinematic problem for the finite radius of the roller (frictional forces and creepage). It is concluded that the contact forces and displacements in the field of contact of all methods show satisfactory results compared to the output obtained from a full-scale model. Comparing the stress and strain state produced in a 1/30 scale twin-disc tests to the full scale wheel/rail experiments calculated by the finite element method [14] concludes that larger disc diameters are beneficial, reducing the influence of surface roughness and wear. The contact mechanics of the rail-vehicle motion is discussed in Ref. [11], presenting the development of the theory of rolling contact. It is concluded that when the traction-slip distribution inside the contact area is significant, Kalker full theory and FASTSIM calculations of the tangential forces and creepages are required to assess wear damage. Calculation of the tangential forces and creepages within the rolling-sliding contact at two-disc testing is discussed in Ref. [12], stressing the importance of preventing excessive profile wear of the two-discs since this will result in the contact pressure to lose its peak at the centre, resulting in the Hertzian theory not to be applicable anymore. With a developing 'ball-groove' conformal contact the use of Hertz + Kalker's FASTSIM code would lead to inaccurate results, requiring e.g. Kalker's NORM + TAN boundary element-based computer code.

The paper outline is the following. After the introduction in chapter one, the test rig design, scaling issues and consequent disc geometry and loading choices in test rig set-up will be discussed within chapter two. Chapter three presents the calculated equivalent Tγ levels with respect to slip ratios (longitudinal and lateral), normal load and friction levels using the FASTSIM algorithm for wheel-rail contact evaluation. The test protocol is presented in chapter four, discussing the control of the operational settings and executed measurements. Within chapter five the resulting RCF development will be presented for the different operational settings, providing the index values required to establish the RCF damage function. Evaluation of the test runs within chapter five also includes metallurgical analysis of the running surfaces, especially the micro-structure deformation levels and the development of the contact conditions. Discussion and conclusions are presented respectively within chapter six and seven.

2. Two-disc machine set-up

All tests have been conducted on the specially developed rolling-sliding two-disc machine at DEKRA Rail. Previous tests on this machine focused on the development of rail surface materials and alternative rail profiles, investigating friction characteristics and their contribution to squeal noise reduction [13]. This machine features two separately driven discs. With the here applied rotational speed in the order of 1000–1100 RPM, the resulting contact speed is 45–50 km/h.

Within Fig. 1 the set-up of the two-disc machine is shown. The rear (rail) disc, including bearings and engine, is mounted on a moveable support. This support is moved by a pneumatic cylinder, through a force transducer, which is in line with the disc-disc contact. Each disc is driven by a separate motor with frequency controller. At one of the driving axles the torque is measured, allowing to determine the
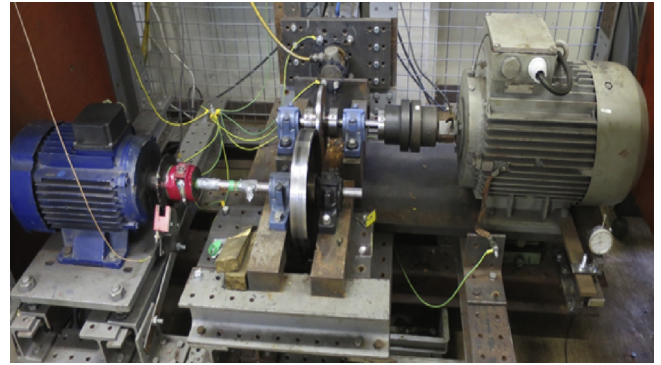
Fig. 1. Two-disc testing machine overview.

tractional effort and thereby the coefficient of friction active between the two discs (see chapter 3). Maintaining a set difference in circumferential speed between the wheel and the rail disc results in a longitudinal slip level. The wheel disc is acting as driving disc (maintaining the higher circumferential speed). Continuously measuring the rotational speed of both discs, a proportional–integral–derivative controller (PID) provides a control loop feedback mechanism to retain the desired longitudinal slip set-point. Measurement error for the torque is ± 3%. The rotational speed is measured with an accuracy of ± 1% however the circumferential velocity can be influenced due to wear. For this reason the diameter of each disc is frequently re-measured.

The applied test rig configuration allows a contact angle to be set to one of the discs introducing lateral slip. Together with the longitudinal slip this simulates the dynamic conditions between wheel and rail when negotiating a curve. Lateral slip can be induced by lifting the support of the moveable disc on one side. This way, an angular difference in the planes of both discs is induced, causing a lateral slip of maximum 2%. During the here performed tests an angular rotation of 2 mrad (0.2% lateral slip) was maintained between the two discs. Initial alignment of the two discs has been carried out with help of a specialist 3-D laser measuring arm, with a specified accuracy of ± 0.013 mm.

2.1. Disc-specimens

The aim of the work is to validate the two-disc approach for RCF-damage function development. The chosen approach is to derive the RCF-damage index values for a rail grade for which the RCF damage function already has been established from field observations; the pearlitic normal rail grade from Ref. [1]. For this purpose rail discs have been manufactured from a normal grade rail type R220 (Fig. 2). Markings have been applied to identify the individual rail disc sections initially located at the head, web and foot of the rail.

The rail disc diameter is 177 mm, the transverse plane is curved (radius 12 mm). The wheel disc is manufactured from medium-carbon steel C 45 (material nr. 1.0503). To improve the shape stability of the running surface the wheel disc has been hardened (heated to 840 °C
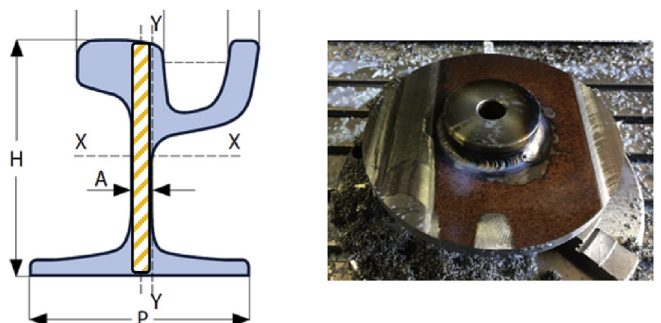
Fig. 2. Rail disc manufactured form a new UIC 59R2 profile rail, grade R220.

than quenched in oil). The transverse plane of the wheel disc diameter is flat. The wheel disc diameter is 240 mm.

3. Contact loading

Regarding the effect of scaling and simulation of the wheel-rail contact Jaschinsky [7] concludes exact similarity of the contact ellipse to be important with respect to the creep forces when these are not saturated. The shape of the contact ellipse is defined by the contact ellipse ratio a/b with a representing half of the contact width and b half of the contact length.

The ratio of the contact ellipses as well as the normal contact stress can be determined by the Hertz theory [11]. The aim is to choose the curvature of the discs together with the normal load in such a way that during testing the resulting contact patch dimensions and normal contact stress correspond to those that occur in track. To this end a representative train-track configuration has been selected which is known to develop RCF damage (Headcheck) in track; a Dutch VIRM intercity vehicle negotiating a 1200 m radius curve. Relevant track and vehicle details are presented in Ref. [2]. The calculated contact ellipse ratio a/b for this track-vehicle configuration, derived from the in Ref. [2] performed train-track simulations, is 2.7 with the mean contact stress being 1050 MPa. The in chapter 2 presented disc curvatures together with disc material properties (elastic modulus and Poisson's ratio) and an applied normal load of 900 N results in an a/b ratio and mean contact stress similar to the calculated vehicle-track reference situation.

The occurring friction coefficient can be calculated from the normal force (Fn), the longitudinal slip and the torque (T). If full slip occurs, the friction coefficient is equal to $\frac{T}{rF_n}$, with r being the radius of the disc. At low (partial) slip the coefficient of friction can be calculated using the Herz + FASTSIM algorithm. This algorithm is used to derive the figure below (Fig. 3), allowing the active coefficient of friction during testing to be determined from the graph.

Starting from the level of friction coefficient, creepages, normal load and disc curvature, the resulting value of wear index Tγ can be calculated using the FASTSIM algorithm [11] for wheel-rail contact evaluation. Since [7] concludes Tγ to scale proportional to the normal force an equivalent Tγ for a full size wheel can be calculated from the Tγ for the two disc set up (Fig. 4).

As explained by Ref. [6] the initiation of surface cracks takes place if
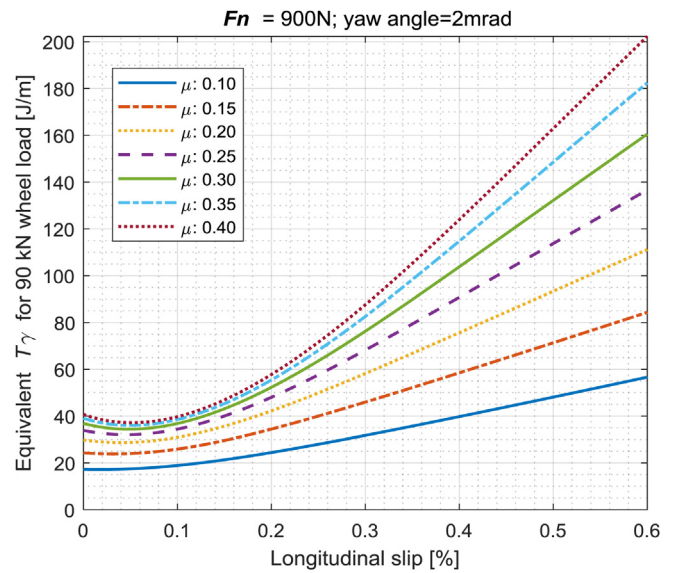
Fig. 4. Equivalent Tγ for 90 kN wheel load as a function of longitudinal slip and friction coefficient. The graph is valid for a set angular rotation between the two discs of 2 mrad.

the surface layer accumulates uni-directional plastic strain higher than the strain to failure. In rolling-sliding contacts, the amount of this accumulation is a function of the coefficient of friction, the maximum contact pressure and the shear yield strength of the material. Tyfour et al. also showed the initiation of fatigue cracks is connected to dry rolling-sliding test runs with relatively high levels of friction, positioning the maximum shear stress at the contact surface. Crack propagation is triggered when subsequent wet rolling-sliding test runs are applied. Due to lubrication the coefficient of friction will drop, relocating the maximum shear stress below the contact surface. At the same time fluid will be trapped within the cracks, stimulating crack propagation due to hydrostatic pressure build up and lubrication of the crack faces, both resulting in increased stresses at the crack tip. Since the purpose of the here performed study is to establish the RCF life as the number of rail-disc cycles required to initiate a fatigue crack only dry rolling-sliding tests have been performed.

4. Testing procedure

Prior to the start of each test run the contact surface roughness of both discs is measured as well as the surface cross sectional profile, after which the surfaces are cleaned using an degreasing agent. To provide initial strain hardening below the contacting surfaces a run-in period of 3000 dry cycles is applied with 1000 N of normal load and zero longitudinal slip. Subsequently longitudinal slip is applied. After the torque/friction has stabilized the resulting coefficient of friction is determined. Based upon the measured coefficient of friction the slip percentages are set and adjusted during testing accordingly to those that the desired Tγ loading value is achieved.

4.1. Assessing RCF-life

The 'RCF damage index' expresses the number of cycles before visible RCF cracks can be expected on the rail head. Burstow [1] suggests, for reasons of feasibility, a minimum surface length of approximately 2 mm, stating that cracks to be visible at this length must have developed beyond the initiation stage and some crack growth must have taken place. Similarly RCF life for the roller rig is defined as the number of rail disc rolling-sliding cycles required to initiate a fatigue crack of a visible length. With the 1:5 scale of the two-disc machine a crack length of 0.40 mm is applied here.

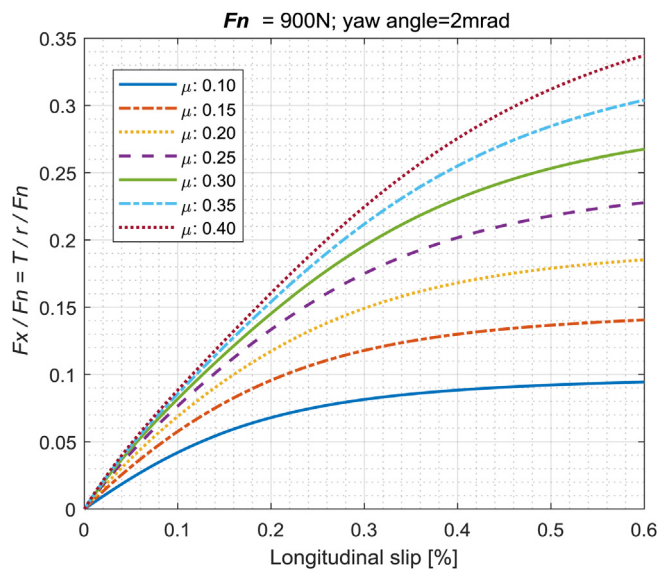**Fig. 3.** Traction force relative to the normal force (Fx/Fn = T/r/Fn) as a function of longitudinal slip and friction coefficient. The graph is valid for a set angular rotation between the two discs of 2 mrad.

4.2. Crack detection/metallographic analysis

During the actual test-run operation the running surface is monitored after every 20.000 rail disc cycles (approx. 15 min of run time). Monitoring of the running surface consists of visual inspection using a stereo microscope. Early crack detection is further supported by Eddy current measurements. During each test run the rotational speed of both discs, the normal load and torque are continuously sampled. Every 100.000 cycles measurements regarding surface roughness and cross profile are repeated. After completion of the full test, surface roughness and profiles are again measured, after which the rail disc can be sectioned and prepared for metallographic analysis and hardness measurements.

5. Results and analysis

Index values with regard to the R220 RCF-damage function have been derived for two loading levels of $T\gamma$. One selected level ($T\gamma = 65$ J/m) is positioned at the peak of the function, marking the transition from the RCF dominated region to the region of mixed RCF-Wear. From Ref. [1] the corresponding index value to this position is 100.000 cycles (Fig. 14). The other test loading level is chosen at $T\gamma = 120$ J/m for which [1] indicates 200.000 cycles to visible RCF damage. Test results at the two applied $T\gamma$ loading levels are summarized in Table 1 and Table 2.

5.1. Surface crack detection

Surface crack development has been visually determined (Fig. 5). Surprisingly cracks at the rail disc running surface are seen to initiate only at the rail disc running surface positioned within the former rail head. At the here tested loading levels no cracks are seen to develop within the disc circumference machined from the rail web or foot area (Fig. 6).

5.2. Running band development

Due to wear and plastic deformation the shape of the rail disc running band is seen to widen during testing. At the $T\gamma$ loading level of 65 J/m the running band maintains a uniform appearance over the circumference of the rail disc. However, during testing at 120 J/m a wavy pattern is seen to appear; a repetitive widening of the contact band. This wavy pattern develops evenly over the rail disc circumference. Again cracks are only seen to appear within the rail disc circumference machined from the rail head. With the formation of this wavy pattern cracks no longer form uniformly over the running band but are seen to form in clusters, suggesting local differences in loading. These patches of cracks appear mainly in the wider parts of the running band however individual cracks are seen also at some of the narrow sections.

Table 2
Testing conditions and results for $T\gamma$ loading level = 120 J/m.

|	Test number	
	1	2
Roughness (Ra) rail/wheel.	Initial:0.25/0.67 End:0.44/0.45	Initial:0.34/0.67 End:0.46/0.45
Friction coefficient, [run nr.]	0.45 [1]/0.29 [2]/ 0.21 [5]/0.20 [11]	0.45 [1]/0.35 [2]/ 0.23 [3]/
Longitudinal slip (%), [run nr]	0.40 [1]/0.50 [2]/ 0.65 [5]/0.65 [11]	0.40 [1]/0.50 [2]/ 0.64 [7]/0.69 [10]
Lateral slip (%)	0.20	0.20
Normal load (N)	900	900
Contact area (mm²) initial/end	0.67/0.88	0.97/1.9
Contact ratio (a/b) initial/end	3.7/2.8	2.4/0.6
RCF life (cycles to visual surface crack length of 0.40 mm)	220.000	200.000
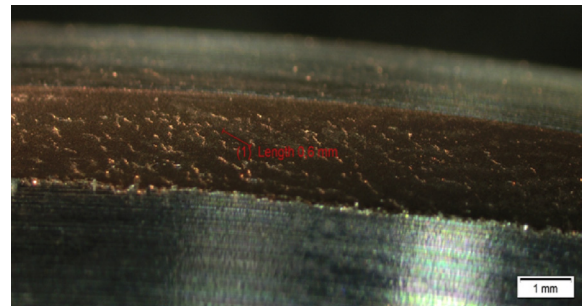
Fig. 5. Rail disc circumference initially located within the rail head area showing cracks at the running surface (load: $T\gamma$ 65 J/m, 280 k cycles). This part of the circumference is further referred to as 'area H'.
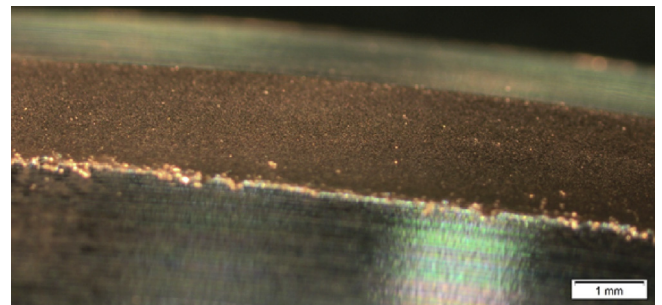

Fig. 6. Rail disc circumference initially located within the rail web area showing no cracks at the running surface (load: $T\gamma$ 65 J/m, 280 k cycles). This part of the circumference is further referred to as 'area W'.

Table 1
Testing conditions and results for $T\gamma$ loading level = 65 J/m.

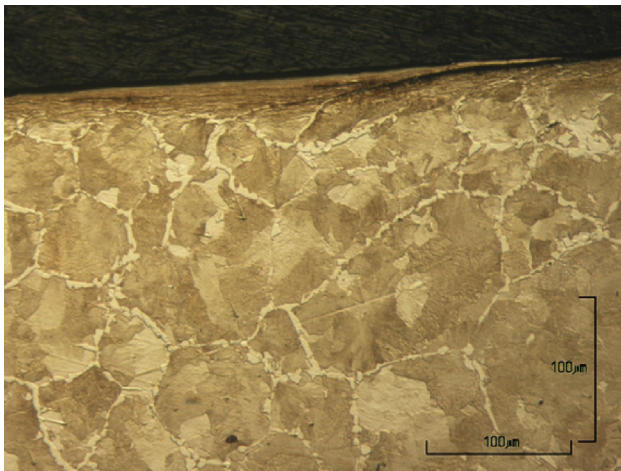|	Test number		
	1	2	3
Roughness (Ra) rail/wheel.	Initial: 0.26/0.69 End: 0.34/0.35	Initial: 0.21/0.66 End: 0.32/0.32	Initial: 0.22/0.62 End: 0.38/0.32
Friction coefficient, [run nr.]	0.40 [1]/0.18 [5]/0.18 [9]/0.18 [13]	0.40 [1]/0.25 [3]/0.23 [5]	0.40 [1]/0.23 [4]/0.22 [6]
Longitudinal slip (%), [run nr]	0.25 [1]/0.42 [5]/0.42 [9]/0.42 [14]	0.25 [1]/0.27 [3]/0.30 [5]	0.25 [1]/0.30 [4]/0.32 [6]
Lateral slip (%)	0.20	0.20	0.20
Normal load (N)	900	900	900
Contact area (mm²) initial/end	0.74/1.29	0.94/1.25	0.96/1.35
Contact ratio (a/b) initial/end	3.0/1.2	2.3/1.4	2.3/1.3
RCF life (cycles to visual surface crack length of 0.40 mm)	0.6 mm crack length after 280.000 cycles	100.000	120.000

Fig. 7. Crack morphology of a flake, longitudinal cross section – area H (load: Tγ 65 J/m, 280 k cycles).

5.3. Metallographic analysis

From the rail disc running surface at area H (head) and area W (web) both longitudinal and lateral cross sections were prepared for metallurgical examination. The morphology of the observed surface cracks at area H is characterized as a 'flake' (Fig. 7). The observed damage is similar to the in Ref. [6] presented damage after only dry cycle testing. Accordingly to Ref. [6] RCF crack development is caused when a dry cycle test sequence is followed by wet rolling sliding cycles. From the rail disc transverse cross section (Fig. 8), the deformation at the running surface as a result from the applied lateral slip can be observed.

The microstructure analysis shows clear differences between the rail disc material from the rail head (H) and rail web (W). Area H possesses a pearlitic structure with a network of ferrite positioned at the pre-austenite grain boundaries. Contrary to the microstructure of area H, the microstructure of transversal cross section of area W shows a significant higher percentage of free ferrite, displaying a dominant orientation (Fig. 9). This orientation is very likely to be the result of the rolling process during rail production. The observed difference in microstructure is reflected by the material hardness, measured at the non-deformed base material. The average micro hardness value at the rail web (W) is 266 HV(500 g) against 300 HV(500 g) at the rail head (H). From the differences in hardness and microstructure a difference in wear behaviour is to be expected. This is confirmed by the executed rail
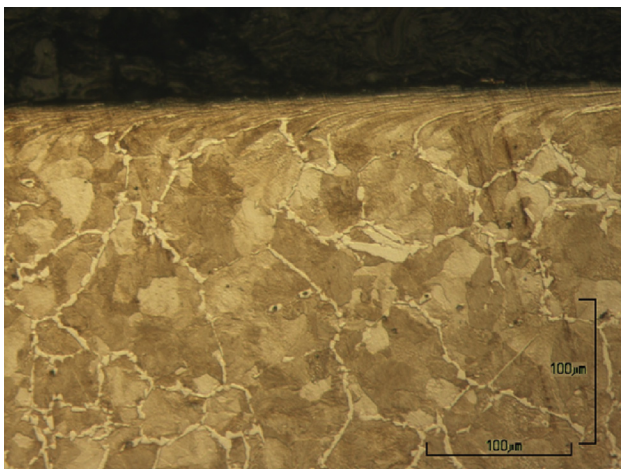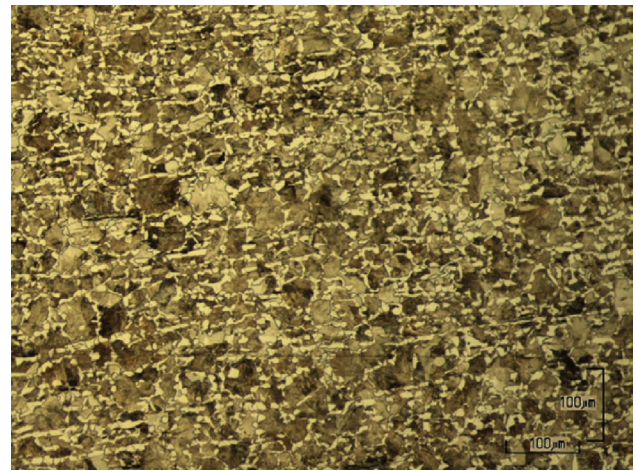

Fig. 9. Microstructure at area 'W'(transverse cross section). The rail web material shows a texture composed of pearlite (brown) and lines of free ferrite (white). (For interpretation of the references to colour in this figure legend, the reader is referred to the Web version of this article.)

disc cross profile measurements, showing a difference in profile wear between the different circumferential sections. After 280 k cycles the measured maximum vertical wear at area H is 0.7 mm against 1.2 mm at area W. The increased wear rate at area W can explain for the absence of cracks in this part of the disc circumference, shifting the damage response within this section into the fully wear dominated regime.

5.4. Contact conditions

From the performed miniprof profile measurements the development of the contacting surfaces has been established. As shown in Fig. 10 the rail disc profile gets flatter and asymmetric. The asymmetry is caused by plastic deformation. It has been confirmed that high part of the profile develops with the direction of slip. The wheel disc does not show any significant change in profile.

Due to the shape of the rail disc profile, the contact pressure distribution and the Tγ cannot be evaluated using FASTSIM. Therefore, Kalker full theory [11] has been applied, using our own Matlab implementation. Figs. 11 and 12 show the resulting contact pressure distribution. It can be seen that the maximum contact pressure decreases
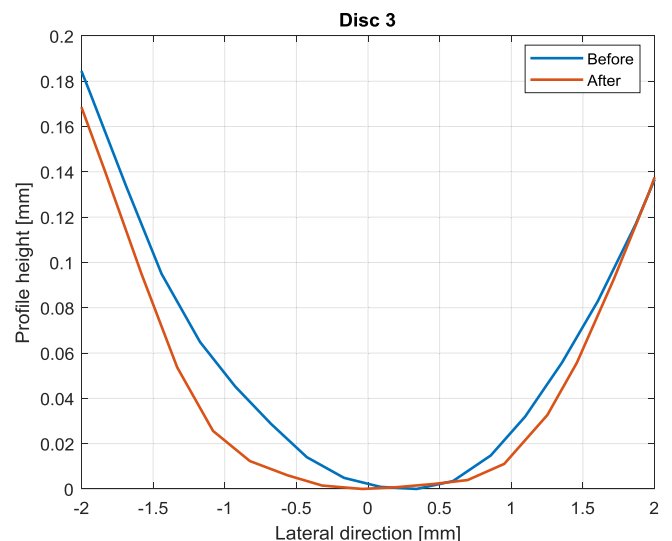

Fig. 8. Transverse cross section over the rail disc running surface, area H (load: Tγ 65 J/m, 280 k cycles).

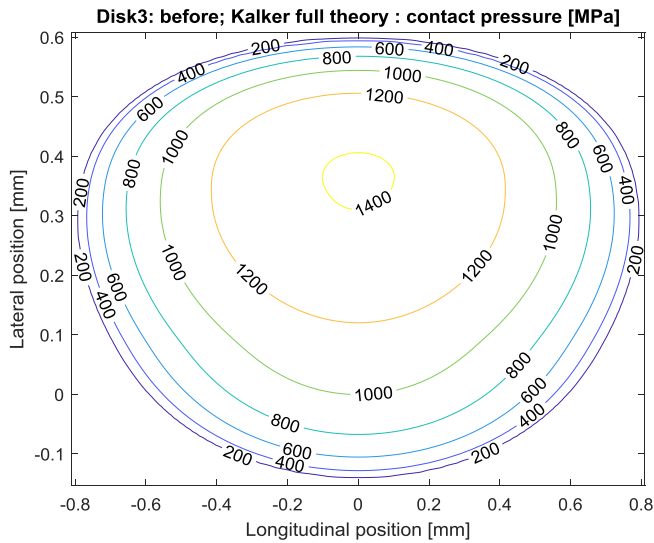**Fig. 10.** The lateral profile of rail disc 3 before and after testing.

Fig. 11. Contact pressure of disc 3 before testing, as calculated using Kalker full theory.
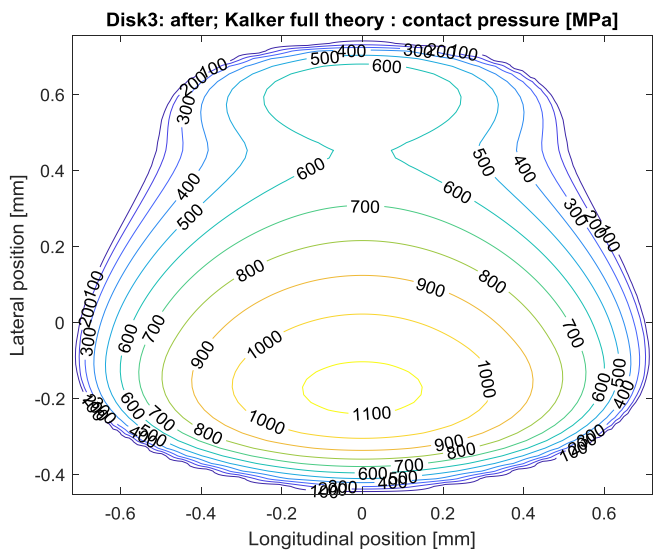

Fig. 12. Contact pressure of disc 3 after testing, as calculated using Kalker full theory.

during testing. However, the equivalent $T\gamma$, as calculated using Kalker full theory, remains unaffected by the change in contact pressure distribution. Therefore Figs. 3 and 4 remain valid and may be used throughout the test for estimating the friction coefficient and calculating the $T\gamma$ at specified settings of the test setup.

5.5. Validation result

Damage function indices for the different $T\gamma$ loading levels have been determined from the observed cycles to the initiation of visual surface cracks with a length of 0.40 mm. The resulting indices are presented in Fig. 13. The RCF damage function of the R220 rail grade as established by Burstow [1] is shown by the black line. For the examined wear numbers (65 and 120 J/m) the rail disc indices established by two-disc testing can observed to be in the same order of magnitude as that of the normal grade rail RCF damage function.

6. Discussion

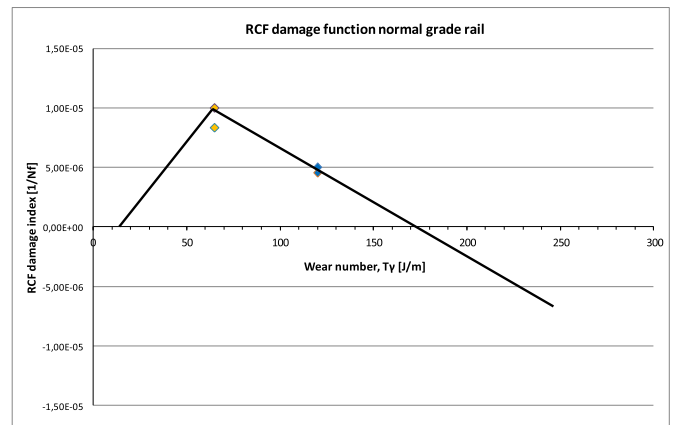RCF and wear behaviour of rail and wheel materials has been

Fig. 13. Damage function indices at loading levels $T\gamma$ 65 and 120 J/m established with two-disc testing, depicted within the RCF damage function of normal grade rail as established by Burstow [1].

studied by means of two-disc testing also in the past. Many of these earlier studies focus on describing the wear behaviour with regard to specific loading conditions, usually applying longitudinal slip only. The aim of this study is to validate a two-disc test approach supporting future description of the full range of the RCF damage function, addressing both the RCF and wear dominated regime. The applied test rig configuration allows a contact angle to be set to one of the discs thus introducing, beside longitudinal slip from the set difference in circumferential speed, also lateral slip to simulate the dynamic conditions between wheel and rail when negotiating a curve.

Regarding test rig design, scaling issues and consequent design and loading choices in the test rig set-up are important especially from the viewpoint of contact patch ratio and normal contact stresses. The curvature of the discs together with the normal load are chosen in a way that the resulting contact patch dimensions, and normal contact stress during testing correspond to those that occur at Headcheck sensitive track locations.

Equivalent $T\gamma$ levels are calculated with respect to slip ratios (longitudinal and lateral), normal load and friction levels using the FASTSIM algorithm for wheel-rail contact evaluation. Depending on the development of the coefficient of friction between the two discs and the targeted value of $T\gamma$ the set longitudinal slip is adjusted. The applied range varied from a minimum value of 0.25% to a maximum of 0.69%. For all executed tests the level of friction coefficient is seen to stabilize at around 0.2 indicating this to be independent of the here applied values of longitudinal slip. Higher values of longitudinal slip are seen to result in an increase of the resulting surface roughness. Due to wear and deformation at the running band the rail disc profile is seen to change during testing. With increasing $T\gamma$ loading level an increase in wear rate can be observed. The equivalent $T\gamma$, as calculated using Kalker full theory, remains unaffected by the observed change in profile and corresponding contact pressure distribution.

Similar to the RCF damage model of Burstow [1] which is based on visual crack length initiation in track, the RCF life for the roller rig is defined as the number of rail disc rolling-sliding cycles required to initiate a fatigue crack of a visible length. With the 1:5 scale of the two-disc machine a crack length of 0.40 mm is applied here.

Machining the disc from a rail resulted in part of the circumference to be positioned at the initial rail head, part in the web and part in the foot to the rail. Unlike the rail disc running surface positioned within the former rail head, the disc circumference from the web area is showing no crack initiation. From the differences in microstructure and hardness between the rail head and rail web material a difference in wear resistance is to be expected. This is confirmed by the executed rail disc cross profile measurements, with web wear rate being 1.7 times that of head wear. The higher wear rate at the web section can explain

for the absence of cracks in this part of the disc circumference, shifting the damage response within this section into the fully wear dominated regime.

For the examined wear numbers (65 and 120 J/m) the RCF damage function indices established by two-disc testing can be observed to be in the same order of magnitude as that of the normal grade rail RCF damage function as established by Burstow [1]. With increased Tγ and related wear loading a wavy pattern is seen to develop at the rail disc. Further investigation is required to understand the full impact of this development regarding testing conditions.

The RCF damage functions have significant engineering relevance. Their application allows for a dedicated rail grade selection, adapted to site-specific operational conditions. They can be used either in plain track and in the design of special parts of the rail network, such as switches and crossings and can be expected to significantly affect the life-cycle costs. The track engineer can use RCF damage functions to optimise track maintenance in relation to RCF generation. From track and traffic characteristics the mean value of the wear number Tγ along a curve or switch can be calculated. From these calculations track location specific Tγ look up tables can be set up. With the applicable RCF damage function, the accumulated fatigue index for the section can be determined from the average daily traffic. This can e.g. support a fit-for-purpose rail grade selection upon renewal. A validated method for a controlled quantitative determination of the RCF damage function will provide a solid base for a future optimisation of rail grade design, selection and maintenance. The two-disc laboratory set up allows RCF index values to be determined with more accuracy and higher resolution compared to field testing. This will allow RCF damage models to be derived with higher resolution, resulting in a more detailed understanding of the RCF behaviour of individual rail grades.

7. Conclusion

RCF-damage function indices have been established using a rolling-sliding two-disc laboratory set up. The applied test rig configuration allows both longitudinal and lateral slip to be introduced into the contact, corresponding to the dynamic conditions between wheel and rail when negotiating a curve. For purpose of laboratory set-up validation, performed tests investigate the damage response of the normal rail grade R220. For this rail grade the RCF-damage function is already available from field observations [1].

For the examined wear numbers the RCF damage function indices established by two-disc testing can be observed to be in the same order of magnitude as that of the normal grade RCF damage function as established from field observations. The validation result suggest that the two-disc approach can be used to support future work to establish RCF-damage functions within a well defined laboratory environment.

8. Future work

Further validation work could aim at Tγ loading levels within the regime of full wear (Tγ > 170 J/m). The development of the running band especially during testing at higher loading levels and how this could affect the loading conditions needs to be further investigated. Two-disc testing can start to determine the RCF damage functions for a range of rail grades, from which the individual contribution towards (track) loading response and related rail grade selection can be appreciated.

The initiation of cracks/flakes during testing is seen to only occur at the rail disc running surface positioned within the former rail head, the disc circumference from the web/foot area showed no crack initiation. This difference in response to loading levels needs to be further investigated.

Acknowledgement

References

[1] M. Burstow, Whole life rail model application and development for RSSB (T115) – continued development of an RCF damage parameter, Engineering Research Programme, Rail Safety & Standards Board, 2004.

[2] M. Hiensch, M. Steenbergen, Rolling Contact Fatigue on premium rail grades: Damage function development from field data, Wear 394–395 (2018) 187–194 https://doi.org/10.1016/j.wear.2017.10.018.

[3] D. Fletcher, J. Beynon, Development of a test machine for closely controlled rolling contact fatigue and wear testing, Journal for Testing and Evaluation, JTEVA 28 (4) (July 2000) 267–275.

[4] M. Ishida, Y. Satoh, Development of rail/wheel high speed contact fatigue testing machine and experimental results, Q. Rep. 29 (2) (May 1988).

[5] R. Lewis, et al., Mapping railway wheel material wear mechanisms and transitions, JRRT328, Proc. IMechE, Part F: J. Rail and Rapid Transit 224 (2010).

[6] W.R. Tyfour, J.H. Benyon, A. Kapoor, Deterioration of rolling contact fatigue life of pearlitic rail steel due to dry-wet rolling sliding line contact, Wear 197 (1996) 255–265.

[7] A. Jaschinsky, On the Application of Similarity Laws to a Scaled Railway Bogie Model, thesis TU Delft (1990).

[8] M. Gretzschel, A. Jaschinski, Design of an active wheelset on a scaled roller rig, Veh. Syst. Dyn. 41 (5) (2004) 365–381, https://doi.org/10.1080/00423110412331300336.

[9] S.D. Iwnicki, A.D. Wickens, Validation of a MATLAB railway vehicle simulation using a scale roller rig, Veh. Syst. Dyn. 30 (3–4) (1998) 257–270.

[10] N. Bosso, Comparison of different scaling techniques for the dynamics of a bogie roller rig, Veh. Syst. Dyn. 37 (sup1) (2016) 514–530, https://doi.org/10.1080/00423114.2002.11666259.

[11] J.J. KaIker, Wheel-rail rolling contact theory, Wear 144 (1991) 243–261.

[12] R. Stock, R. Pippan, RCF and wear in theory and practice—the influence of rail grade on wear and RCF, Wear 271 (2011) 125–133.

[13] Hiensch, M. Dirks, B. Horst, J. van der Stelt, J, Rail Head Optimisation to Reach a Sustainable Solution Preventing Railway Squeal Noise, Inter-Noise, Istanbul, 2007 2007.

[14] M. Kráčalík, G. Trummer, W. Daves, Application of 2D finite element analysis to compare cracking behaviour in twin-disc tests and full scale wheel/rail experiments, Wear (2016) 346–347.

[15] W.R. Tyfour, J.H. Beynon, The effect of rolling direction reversal on fatigue crack morphology and propagation, Tribol. Int. 27 (1994) 273–282.

[16] Y.B. Huang, L.B. Shi, X.J. Zhao, et al., On the formation and damage mechanism of rolling contact fatigue surface cracks of wheel/rail under the dry condition, Wear 400–401 (2018) 62–73.

[17] W. Daves, W. Kubin, S. Scheriau, et al., A finite element model to simulate the physical mechanisms of wear and crack initiation in wheel/rail contact, Wear 366–367 (2016) 78–83.